bioRxiv preprint doi: https://doi.org/10.1101/360305; this version posted July 2, 2018. The copyright holder for this preprint (which was not certified by peer review) is the author/funder, who has granted bioRxiv a license to display the preprint in perpetuity. It is made available under aCC-BY-NC-ND 4.0 International license.

Beyond members of the Flaviviridae family, sofosbuvir also inhibits chikungunya virus replication

Running Title: Chikungunya is susceptible to sofosbuvir

André C. Ferreira[1,2,7#], Patrícia A. Reis[1#], Caroline S. de Freitas[1,7,#], Carolina Q. Sacramento[1,7,#], Lucas Villas Bôas Hoelz[3,#], Mônica M. Bastos[3], Mayara Mattos[1,7], Erick Correia Loiola[4], Pablo Trindade[4], Yasmine Rangel Vieira[2,7], Giselle Barbosa-Lima[2], Hugo C. de Castro Faria Neto[1], Nubia Boechat[3], Stevens K. Rehen[4,5], Karin Brüning[6], Fernando A. Bozza[1,2], Patrícia T. Bozza[1] and Thiago Moreno L. Souza[1,2,7,*]

[#]- These authors contributed equally as first authors.

Affiliations:

1 – Laboratório de Imunofarmacologia, Instituto Oswaldo Cruz (IOC), Fundação Oswaldo Cruz (Fiocruz), Rio de Janeiro, RJ, Brazil.

2 – Instituto Nacional de Infectologia (INI), Fiocruz, Rio de Janeiro, RJ, Brazil.

3 – Instituto de Tecnologia de Fármacos (Farmanguinhos), Fiocruz, Rio de Janeiro, RJ, Brazil.

4 – D'Or Institute for Research and Education (IDOR), Rio de Janeiro, RJ, Brazil.

5 – Centro de Ciências da Saúde, Universidade Federal do Rio de Janeiro, Rio de Janeiro, RJ, Brazil.

6 – BMK Consortium: Blanver Farmoquímica Ltda; Microbiológica Química e FarmacêuticaLtda; Karin Bruning & Cia. Ltda, Brazil

7 - National Institute for Science and Technology on Innovation on Diseases of Neglected Populations (INCT/IDPN), Center for Technological Development in Health (CDTS), Fiocruz, Rio de Janeiro, RJ, Brazil.

bioRxiv preprint doi: https://doi.org/10.1101/360305; this version posted July 2, 2018. The copyright holder for this preprint (which was not certified by peer review) is the author/funder, who has granted bioRxiv a license to display the preprint in perpetuity. It is made available under aCC-BY-NC-ND 4.0 International license.

***Correspondence footnote:**

Thiago Moreno L. Souza, PhD

****

Fundação Oswaldo Cruz

Centro de Desenvolvimento Tecnológico em Saúde (CDTS)

Instituto Oswaldo Cruz (IOC)

Pavilhão Osório de Almeida, sala 16

Av. Brasil 4365, Manguinhos, Rio de Janeiro - RJ, Brasil, CEP 21060340

Tel.: +55 21 2562-1311

Email: tmoreno@cdts.fiocruz.br

bioRxiv preprint doi: https://doi.org/10.1101/360305; this version posted July 2, 2018. The copyright holder for this preprint (which was not certified by peer review) is the author/funder, who has granted bioRxiv a license to display the preprint in perpetuity. It is made available under aCC-BY-NC-ND 4.0 International license.

Abstract: Chikungunya virus (CHIKV) causes a febrile disease associated with chronic arthralgia, which may progress to neurological impairment. Chikungunya fever (CF) is a consolidated public health problem, in tropical and subtropical regions of the world, where control of CHIKV vector, mosquitos of the *Aedes* genus, failed. Since there is no vaccine or specific treatment against CHIKV, infected patients receive only palliative care to alleviate pain and arthralgia. Thus, drug repurposing is necessary to identify antivirals against CHIKV. Recently, the structure and activity of CHIKV RNA polymerase was partially resolved, revealing similar aspects with the enzyme counterparner on other positive sense RNA viruses, such as members of the Flaviviridae family. We then evaluated if sofosbuvir, clinically approved against hepatitis C virus RNA polymerase, which also aims to dengue, Zika and yellow fever viruses replication, would inhibit CHIKV replication. Indeed, sofosbuvir was 5-times more selective in inhibiting CHIKV production in human hepatoma cells than ribavirin, a pan-antiviral drug. Although CHIKV replication in human induced pluripotent stem cell (iPS)-derived astrocytes was less sensitive to sofosbuvir's, compared to hepatoma cells – this drug still impaired virus production and cell death in a MOI-dependent manner. Sofosbuvir also exhibited antiviral activity *in vivo*, by preventing CHIKV-induced paw oedeme in adult mice, at 20 mg/kg/day, and mortality on neonate mice model, at 40 and 80 mg/kg/day. Our data demonstrates that a prototypic alphavirus, CHIKV, is also susceptible to sofosbuvir. Since this is a clinically approved drug, it could pave the way to become a therapeutic option against CF.

Keywords: chikungunya, chikungunya virus, arthralgia, antiviral, sofosbuvir, drug

bioRxiv preprint doi: https://doi.org/10.1101/360305; this version posted July 2, 2018. The copyright holder for this preprint (which was not certified by peer review) is the author/funder, who has granted bioRxiv a license to display the preprint in perpetuity. It is made available under aCC-BY-NC-ND 4.0 International license.

1. Introduction

Chikungunya virus (CHIKV) is a member of the *Togaviridae* family, genus alphavirus, which causes febrile debilitating illness associated with arthralgia and skin rash (1). Although prolonged and debilitating joint pain and oedema differentiate CHIKV infection among contemporary arboviruses, like dengue (DENV) and Zika (ZIKV) viruses, most often these agents display similar clinical signs and symptoms during the early phase of infection (1). Severe outcomes of CHIKV infection, leading to acute and convalescent neurological impairment, have also been described (2, 3).

Chikungunya fever (CF) is a consolidated public health problem with substantial impact in tropical and subtropical regions of the world, where *Aedes* spp mosquitoes are prevalent and control measures failed (1). In last 5 years, the Americas, African and Eurasian regions have been severely impacted by CHIKV (4). For instance, in Brazil, since 2014, the Asian and East-Central-South-African (ECSA) genotypes of CHIKV co-circulate (5-7), highlighting a substantial viral activity in a country historically hyperendemic for DENV. Since no specific treatment or vaccine against CHIKV exist, repurposing of clinically approved drugs, preferentially aiming a viral target, is a necessary response against CF.

CHIKV has a positive-sense single-stranded 11.8 kilobase RNA genome, which encodes four non-structural (nsP1-4) and five structural proteins (C, E1, E2, E3 and 6K) (8). Among these proteins, nsP4 encodes for the viral RNA-dependent RNA polymerase (RDRP).Recently, nsP4 structure was partially resolved (9). As other RNA polymerases from positive sense RNA viruses, CHIKV nsP4 possesses well-conserved motifs, such as D-x(4,5)-D and GDD, spatially juxtaposed, wherein Asp binds Mg_2+ and Asn selects ribonucleotide triphosphates over dNTPs, determining RNA synthesis (10). Moreover, since the RDRP activity is absent on host cells, it constitutes a suitable target for antiviral intervention.

We, and others, have demonstrated that sofosbuvir, a clinically approved against hepatitis C virus (HCV) (11-13), also inhibits the replication of flaviviruses, like ZIKV, DENV and yellow fever virus (YFV) (14-19). Sofosbuvir is a safe and a well-tolerated drug, from 400 to 1200 mg daily in 24 weeks regimen. Sofosbuvir is a uridine monophosphate prodrug that requires the removal of the phosphate protections to enter a pathway that yields sofosbuvir triphosphate, the pharmacological active compound as antiviral (11). Although hepatic cells have the most effective system to remove sofosbuvir's phosphate protections,

bioRxiv preprint doi: https://doi.org/10.1101/360305; this version posted July 2, 2018. The copyright holder for this preprint (which was not certified by peer review) is the author/funder, who has granted bioRxiv a license to display the preprint in perpetuity. It is made available under aCC-BY-NC-ND 4.0 International license.

functional assays reveals that other cells, relevant for arboviruses infection, may also activate sofosbuvir (11, 16, 20). As expected for a nucleotide analogue, sofosbuvir inhibit the RNA polymerase from different members of the Flaviviridae family, HCV, ZIKV, DENV, YFV (14-19). The conservation of RDRP domain of CHIKV nsP4, when compared to other viral RNA polymerases, led us to hypothesized that CHIKV could also be susceptible to sofosbuvir. Indeed, we originally demonstrated, by cellular assays and animal models, that CHIKV is susceptible to sofosbuvir.

2. Results

2.1. CHIKV RNA polymerase, nsP4, as the predictive target for sofosbuvir.

We considering the homology among viral RDRP to evaluate whether sofosbuvir docks on CHIKV RNA polymerase. For comparisons, the binding mode of sofosbuvir-triphosphate (SFV) and the natural substrate, UTP, were analyzed on the nsP4 model. Three docking simulations for each ligand (totalizing 30 poses per ligand) were carried out. The poses with the lowest energy was selected for analysis (Table 1 and Figure 1). SFV and UTP have similar modes of interaction, but different energy values, respectively, -78.41 and -108.78 arbitrary units (a.u.) (with respect to MolDock scores) (Table 1). Moreover, SFV interacted via H-bonds with Asn348, Ile369, Gly370, Asp371, and Cys411 (H-bond energy = -6.97 a.u.), whereas UTP formed H-bonds with Asn348, Ile369, and Gly370 (bond energy = -3.11 a.u.) (Table 1 and Figure 1). Both SFV and UTP also formed electrostatic attractive interactions with the two Mg^{2+} ions and repulsive interactions with Asp371. Consequently, SFV and UTP displayed electrostatic interaction energies of -117.12 a.u. and -112.84 a.u., respectively (Table 1 and Figure 1). SFV and UTP use similar amino acid residues for steric interactions Phe280, Asn344, Asn348, Ala367, Phe368, Ile369, Asp371, Asp372, Asn373, Ile374, and Cys411, resulting in energies equal to -24.50 a.u and 48.76 a.u, respectively. Nevertheless, minor differences with respect to steric interaction were observed: SFV docks onto Thr345 and Phe410, whereas UTP interacts with Leu250 and Phe251.

bioRxiv preprint doi: https://doi.org/10.1101/360305; this version posted July 2, 2018. The copyright holder for this preprint (which was not certified by peer review) is the author/funder, who has granted bioRxiv a license to display the preprint in perpetuity. It is made available under aCC-BY-NC-ND 4.0 International license.

132 **Table 1: Summary of the interactions of SFV and UTP to nsP4 model of CIKV**.

#	nsP4 model of CHIKV						
	H-bond energy	Residues (H-bond)	Electrostatic Interaction energy	Residues and Co-Factor (Electrostatic)	Steric interaction energy by PLP[b]	Residues and Co-Factor (Steric)	MolDock score
SFV	-6.97[a]	Asn348, Ile369, Gly370, Asp371, Cys411	-117.24	Asp371, Mg^{2+}	-24.50	Phe280, Asn344, Thr345, Asn348, Ala367, Phe368, Ile369, Gly370, Asp371, Asp372, Asn373, Ile374, Phe410, Cys411	-78.41
UTP	-3.11	Asn348, Ile369, Gly370	-112.84	Asp371, Mg^{2+}	-48.76	Leu250, Phe251, Phe280, Asn344, Thr345, Asn348, Ala367, Ile369, Gly370, Asp371, Asp372, Asn373, Ile374, Cys411	-108.78

133 [a] Arbitrary units; [b]Piecewise linear potential(21).

bioRxiv preprint doi: https://doi.org/10.1101/360305; this version posted July 2, 2018. The copyright holder for this preprint (which was not certified by peer review) is the author/funder, who has granted bioRxiv a license to display the preprint in perpetuity. It is made available under aCC-BY-NC-ND 4.0 International license.

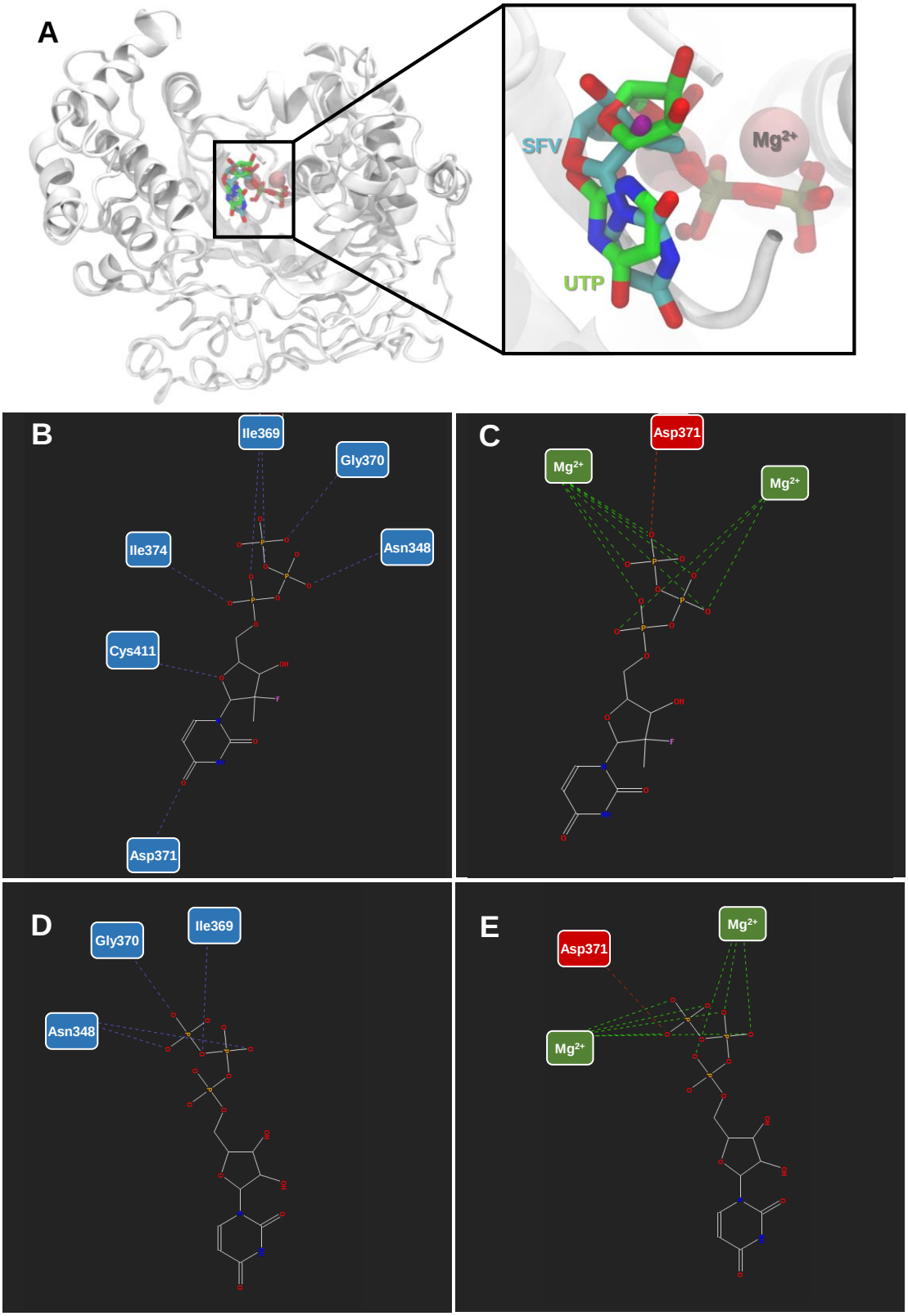

Figure 1. Sofosbuvir triphosphate and nsP4 interactions. (A) Structural representation of the nsP4 model of CHIKV and its interaction with SFV and UTP. Hydrogen bonds and electrostatic interactions between (B; C) SVF and (D; F) UTP, and nsP4 model of CHIKV. The interactions are represented by blue (H-bonds), green (attractive electrostatic interactions), and red (repulsive electrostatic interactions) interrupted lines. The nitrogen atoms are shown in blue, oxygen in red, fluor in pink, and the carbon chain in gray.

bioRxiv preprint doi: https://doi.org/10.1101/360305; this version posted July 2, 2018. The copyright holder for this preprint (which was not certified by peer review) is the author/funder, who has granted bioRxiv a license to display the preprint in perpetuity. It is made available under aCC-BY-NC-ND 4.0 International license.

2.2. CHIKV is susceptible to sofosbuvir *in vitro*

To evaluate if sofosbuvir is indeed endowed with anti-CHIKV activity, phenotypic antiviral assays were performed in human cells previously associated to peripheral virus replication and invasion of the nervous system (22), respectively, hepatoma (Huh-7) and astrocytes derived from induced pluripotent stem (iPS) cells. Supernatants from these infected cultures were harvested and tittered in Vero cells. We observed a dose-dependent inhibition of CHIKV production in hepatoma cells (Figure 2 and Table 2), which is known to possess the machinery to convert the sofosbuvir prodrug to the pharmacologically active metabolite (12). Sofosbuvir was two-fold more potent and 25 % less cytotoxic than ribavirin (Table 2). Consequently, selectivity index (SI) for sofosbuvir was almost five-fold better than for ribavirin, a pan-antiviral drug. Moreover, astrocytes succumb to CHIKV infection in a multiplicity of infection (MOI)-dependent manner, and sofosbuvir partially prevented cell mortality (Figure 3A). Accordingly, sofosbuvir decreased CHIKV replication on astrocytes by 50 % at MOI of 1 (Figure 3B).

bioRxiv preprint doi: https://doi.org/10.1101/360305; this version posted July 2, 2018. The copyright holder for this preprint (which was not certified by peer review) is the author/funder, who has granted bioRxiv a license to display the preprint in perpetuity. It is made available under aCC-BY-NC-ND 4.0 International license.

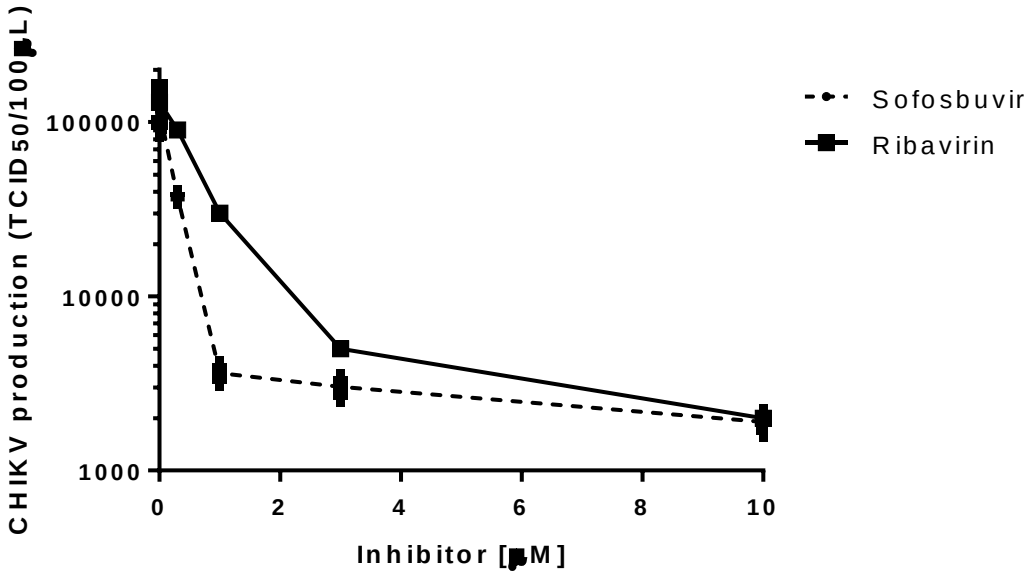

Figure 2 - Pharmacology of Sofosbuvir against CHIKV. Huh-7 were infected with CHIKV at MOI of 0.1 and exposed to various concentrations of sofosbuvir or ribavirin for 24 h. Supernatant was harvested and tittered in Vero cells by $TCID_{50}$/mL. The data represent means ± SEM of three independent experiments.

Table 2 – Pharmacological parameters associated to drug inhibition of CHIKV replication

Drug	EC_{50} (µM)	CC_{50} (µM)	SI*
Sofosbuvir	0.8 ± 0.08	402 ± 32	502
Ribavirin	1.9 ± 0.3	298 ± 22	157

***SI – Selectivity Index (CC_{50}/EC_{50})**

bioRxiv preprint doi: https://doi.org/10.1101/360305; this version posted July 2, 2018. The copyright holder for this preprint (which was not certified by peer review) is the author/funder, who has granted bioRxiv a license to display the preprint in perpetuity. It is made available under aCC-BY-NC-ND 4.0 International license.

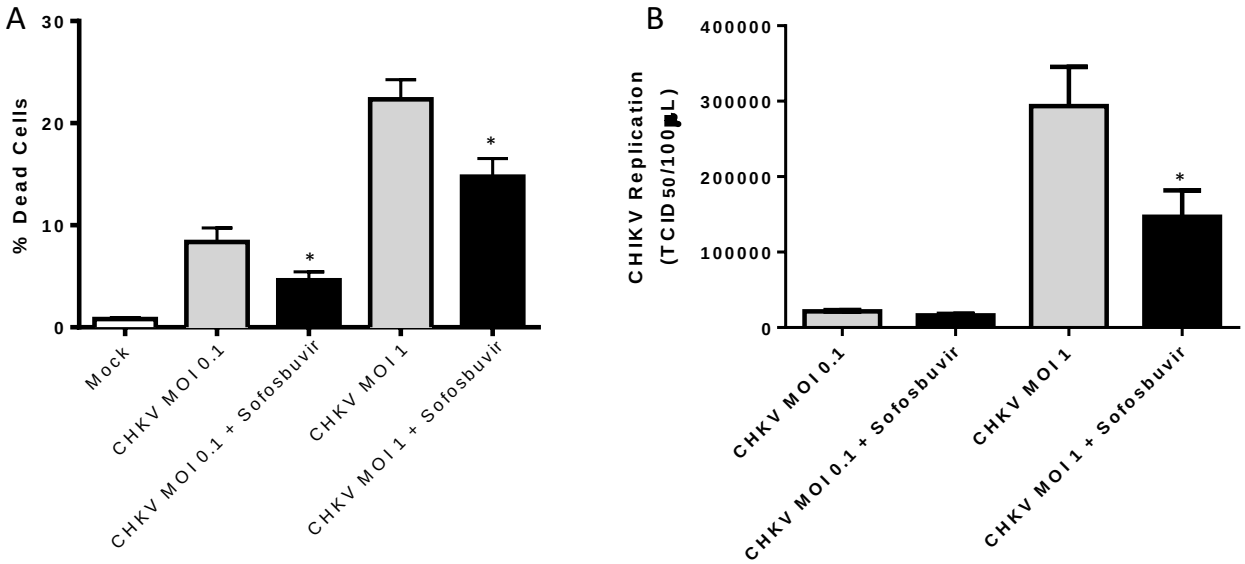

Figure 3 – Sofosbuvir inhibits CHIKV replication in human iPS cell-derived astrocytes. Astrocytes were infected at the indicated MOIs and treated with sofosbuvir at 10 µM. After 5 days, cells were labeled for activated caspase-3/7 and propidium iodide (A) and virus in the supernatant tittered in Vero cells (B). The data represent means ± SEM of three independent experiments performed with five technical replicates. *$P < 0.05$ for the comparison between the infected untreated (gray bars) and treated (black bars) groups.

bioRxiv preprint doi: https://doi.org/10.1101/360305; this version posted July 2, 2018. The copyright holder for this preprint (which was not certified by peer review) is the author/funder, who has granted bioRxiv a license to display the preprint in perpetuity. It is made available under aCC-BY-NC-ND 4.0 International license.

Sofosbuvir protected CHIKV-infected mice, using models of arthralgia and severe infection.

To analyze whether *in vitro* results translate into a systemic protection, we treated CHIKV-infected mouse with sofosbuvir. Initially, treatment was performed in the arthralgia mouse model, in which sofosbuvir was given orally (20 mg/kg/day) one-hour prior to the injection of $2x10^4$ $TCID_{50}$ into the right rind paw. We observed that early after infection paw oedema did not ameliorate with sofosbuvir, suggesting that this drug had now effect on the swelling associated with the insult caused by the injection (Figure 4A-C). Importantly, in the untreated and infected mice, paw oedema was more intense in the following days, whereas the treated animals displayed no differences to mock-infected mice (Figure 4D-F and Figure 5).

bioRxiv preprint doi: https://doi.org/10.1101/360305; this version posted July 2, 2018. The copyright holder for this preprint (which was not certified by peer review) is the author/funder, who has granted bioRxiv a license to display the preprint in perpetuity. It is made available under aCC-BY-NC-ND 4.0 International license.

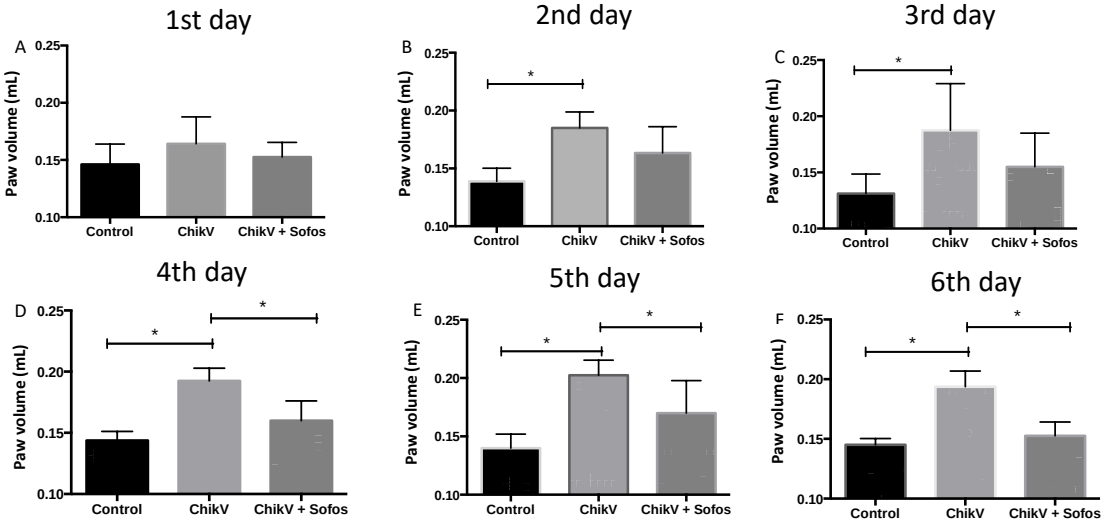

Figure 4. Sofosbuvir ameliorates CHIKV-induced paw oedema. Male Swiss Webster mice (20-25 g) received RPMI medium (Control) or 10^4 $TCID_{50}$ of CHIKV into 50 µl per paw in the ventral side of the right hind foot. Oral treatment with sofosbuvir (sofos) (20 mg/kg/day) started one hour prior to infection. Panels A to F indicates the days after infection, from the first to the sixth, when paw volume was measured in the hydropletismometer. Paw oedema is interpreted by the increase in paw volume over control in the *p<0.05 Tukey's multiple comparisons test (n=8/group).

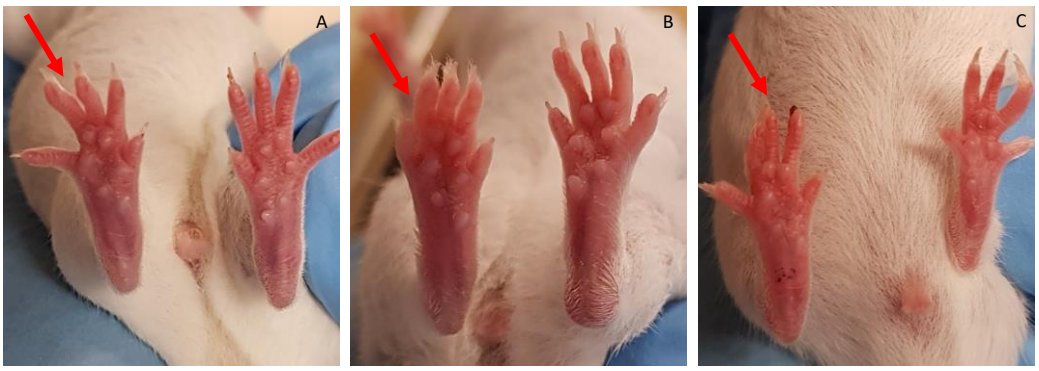

Figure 5. Representative CHIKV-associated paw oedema and sofosbuvir's antiviral effect on the 6th day after infection. (A) Control, (B) CHIKV and (C) CHIKV + sofosbuvir. Arrows indicate the infected paw.

bioRxiv preprint doi: https://doi.org/10.1101/360305; this version posted July 2, 2018. The copyright holder for this preprint (which was not certified by peer review) is the author/funder, who has granted bioRxiv a license to display the preprint in perpetuity. It is made available under aCC-BY-NC-ND 4.0 International license.

Subsequently, we studied sofosbuvir's ability to enhance the survival of CHIKV-infected neonatal mice. Three days-old Swiss mice were infected with CHIKV ($2x10^5$ $TCID_{50}$) intraperitoneally. Treatment was carried out daily, initially with 20 mg/kg, also by intraperitoneal injection, beginning at one day prior to infection (pre-treatment) or on second day after infection (late-treatment). Although pre-treatment doubled the mean time of survival (T_{50}) when compared to mock-infected animals, all infected mice deceased after 6 days of infection (Figure 6A). Late-treatment had marginal contribution to enhance the T_{50} of mice survival (Figure 6A). Of note, post-natal development of the infected mice varied only marginally among the groups (Figure 6B). Under the same experimental conditions of infection, we next performed pre-treatments with different doses of sofosbuvir . Doses of 40 and 80 mg/kg/day doubled and tripled the percentage of animal survival (Figure 6C). At 80 mg/kg/day animals post-natal development were significantly superior to the infected controls (Figure 6D).

bioRxiv preprint doi: https://doi.org/10.1101/360305; this version posted July 2, 2018. The copyright holder for this preprint (which was not certified by peer review) is the author/funder, who has granted bioRxiv a license to display the preprint in perpetuity. It is made available under aCC-BY-NC-ND 4.0 International license.

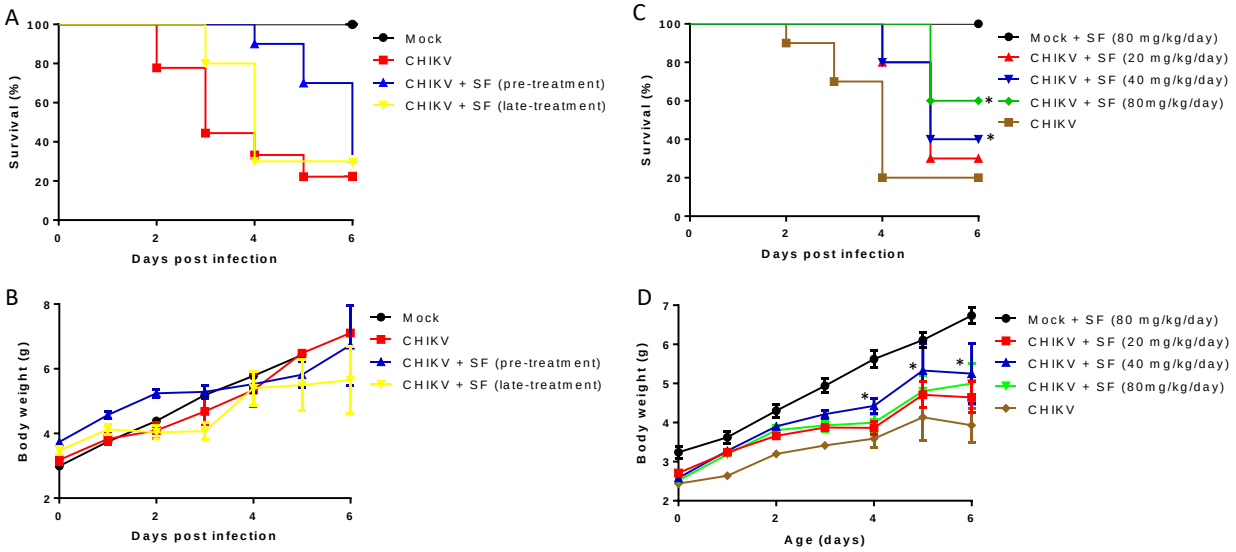

Figure 6. Sofosbuvir, at concentrations of 40 and 80 mg/kg/day, increases survival and inhibits weight loss of CHIKV-infected mice. Three-day-old Swiss mice were infected with CHIKV ($2x10^5$ $TCID_{50}$) and treated with sofosbuvir (SF) either 1 day before (pre-treatment) or 2 days after infection (late-treatment). Survival (A and C) and weight variation (B and D) were assessed during the course of treatment. Panels A and B represent experiments of both pre- and late-treatment with sofosbuvir at 20 mg/kg/day. Panels C and D represent pre-treatment with indicated concentrations of sofosbuvir. Survival was statistically assessed by Log-rank (Mentel-Cox) test. Differences in weight are displayed as the means ± SEM, and two-way ANOVA for each day was used to assess the significance. Independent experiments were performed with at least 10 mice/group (n = 30). * $P < 0.01$.

bioRxiv preprint doi: https://doi.org/10.1101/360305; this version posted July 2, 2018. The copyright holder for this preprint (which was not certified by peer review) is the author/funder, who has granted bioRxiv a license to display the preprint in perpetuity. It is made available under aCC-BY-NC-ND 4.0 International license.

Since some infected and untreated animals survived from experiments described in Figures 6, we evaluated if they had neuromotor sequelae and compared to treated survivors. Animals were held in a supine position with all four paws facing up, and then released. The time to flip over onto its stomach with all four paws touching the surface was measured, as proxy of neuromotor function. CHIKV-infected mice took a median time of 10-20 second to get to the upright position, whereas mock-infected animals did it immediately (Figure 7). Importantly, CHIKV-infected and sofosbuvir pre-treated animals did not present neuromotor sequela, meaning that these animals are healthier than infected controls (Figure 7). Of note, although the late-treatment diminished the median time associated with neuromotor sequela, some animals displayed a behaviour similar to CHIKV-infected animals, making these groups statistically indistinguishable. Altogether, our data suggests that sofosbuvir also inhibits CHIKV replication *in vivo*, ameliorating animals' arthralgia, enhancing survival and preserving neuromotor function.

bioRxiv preprint doi: https://doi.org/10.1101/360305; this version posted July 2, 2018. The copyright holder for this preprint (which was not certified by peer review) is the author/funder, who has granted bioRxiv a license to display the preprint in perpetuity. It is made available under aCC-BY-NC-ND 4.0 International license.

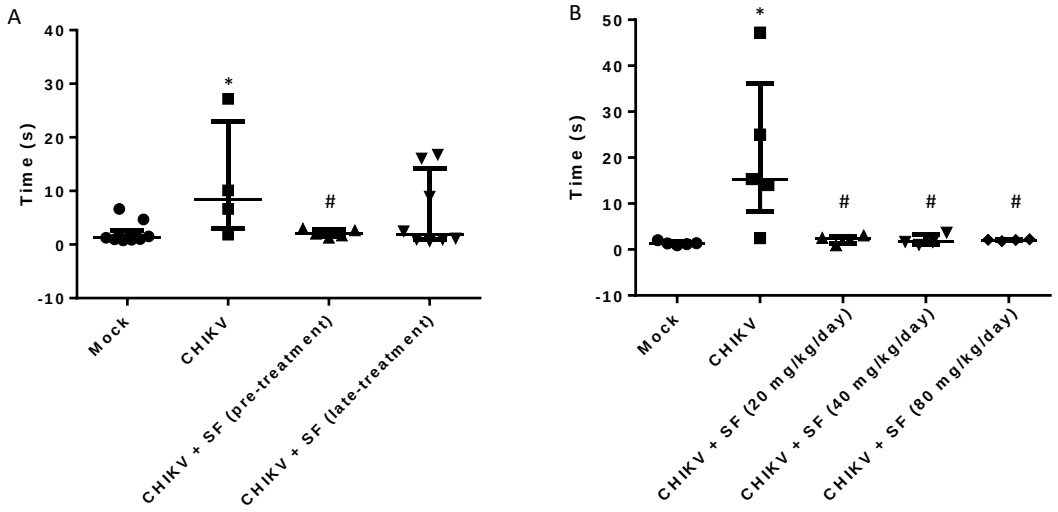

Figure 7. Sofosbuvir prevents neuromotor impairment in CHIKV-infected mice. Three-day-old Swiss mice were infected with CHIKV (2 x 10^5 $TCID_{50}$) and treated with sofosbuvir (SF) beginning 1 day before infection (pre-treatment) or on the 2nd day after infection (late-treatment). (A) Treatment was performed with 20 mg/kg/day. (B) Pre-treatment was performed with indicated concentrations. At the sixth day after infection, animals were turned backwards and allowed up to 60 s to return to the upright position. The results are presented as the means ± SEM. This was a routine measure and at least 10 animals per group were analysed. Student's t test was used to compare untreated CHIKV-infected mice with other groups individually. * $P < 0.01$ mock- vs CHIKV-infected animals. # $P < 0.01$ untreated vs treated animals.

bioRxiv preprint doi: https://doi.org/10.1101/360305; this version posted July 2, 2018. The copyright holder for this preprint (which was not certified by peer review) is the author/funder, who has granted bioRxiv a license to display the preprint in perpetuity. It is made available under aCC-BY-NC-ND 4.0 International license.

3. Discussion

CHIKV is among the reemergent arboviruses in the early 21st century. Although firstly characterized in the 1950's in Tanzania (23), since the 2000's CHIKV activity increased worldwide and reached the new world (24). CF is estimated to cause disability-adjusted life years (DALYs) lost around 45.26 per million people (25). In Brazil, CHIKV was introduced during 2014 (6, 7), when Asian genotype was confirmed in the North Region of Brazil (Oiapoque, Amapá state) and ECSA genotype was identified in the Northeastern region of Brazil (Feira de Santana, Bahia state). The ECSA genotype was subsequently detected throughout Brazil. To the best of our knowledge, Brazil is a rarely case where two genotypes of CHIKV co-circulate. Since early 2016 (summer in the southern hemisphere), DENV, ZIKV and CHIKV co-circulate in Americas, and CHIKV became the most prevalent arbovirus in Brazilian overcrowded cities, like Rio de Janeiro (26). Due to absence of vaccine and specific antiviral treatment, CHIKV prevention depends basically on vector control, whereas patients with CF receive palliative care with nonsteroidal anti-inflammatory drugs (NSAIDs) or corticoids depending on phase of the disease (27).

CHIKV possesses a complex and not fully understood pathogenesis, virus replicate in peripheral organs and may invade the nervous system and synovial fluid (22, 28). Recent efforts to identify substances against CHIKV were carried out, leading to the discovery of chloroquine (29), berberine, abamectin and ivermectin (30). Among these substances, ivermectin was shown to inhibit Flaviviruses NS3 helicase activity (31). By analogy, this drug may also target a CHIKV protein, like nsp2 – which seems to possesses an helicase activity (32). The other identified compounds, such as the alkaloid berberine, target cellular rather than viral pathways (33). We, and others, have shown that sofosbuvir is endowed with antiviral activity against flaviviruses (15-17). The recent advances in the CHIKV nsP4 RDRP core domains structure and function highlighted to the presence of conserved motifs among RNA polymerases from positive-sense RNA viruses (9). Indeed, sofosbuvir docked onto CHIKV nsP4 using conserved amino acid residues, also required for binding of UTP, the natural substrate. Sofosbuvir inhibited CHIKV replication in human hepatoma cells. These cells were used because they represent one of the most efficient *in vitro* models to convert sofosbuvir to the active metabolite and liver is a relevant organ for CHIKV pathogenesis (22, 28). Growing evidence indicates that CHIKV may impair neurological function, by directly invading the nervous

bioRxiv preprint doi: https://doi.org/10.1101/360305; this version posted July 2, 2018. The copyright holder for this preprint (which was not certified by peer review) is the author/funder, who has granted bioRxiv a license to display the preprint in perpetuity. It is made available under aCC-BY-NC-ND 4.0 International license.

system (28, 34, 35). We used a sophisticated human iPS-derived astrocyte culture to show that sofosbuvir inhibits CHIKV replication and virus-associated cell mortality, although in lesser effective manner when compared to huh-7 cells. Accordingly, in the neonatal mouse model of CHIKV infection, sofosbuvir enhanced animal survival at doses higher than required to produce the same effect on ZIKV-infected pups (16). Consistently, sofosbuvir is safe to be used clinically up to 1200 mg per day (12). With respect to the time frame of opportunity to treat CHIKV-infected mice, a narrow window was observed – similarly to what we have noticed towards ZIKV (36). In other acute virus infections, like influenza, mortality is dramatically reduced when neuraminidase inhibitors are administered early in the time course of infection, such as within 2.5 days of infection (37). The identification of individuals at higher risk, to receive sofosbuvir prophylactically, or very early after infection represent one of the challenges to translate our date into public health intervention.

Moreover, we observed that, at experimental infection conditions milder than required for animal mortality, sofosbuvir, at reference dose for pre-clinical studies, 20 mg/kg/day (13), protected arthralgia-related paw oedema. Thus, it is important to further study whether sofosbuvir could act synergistically with anti-inflammatory drugs to improve the quality of life for patients with CHIKV-associated chronic arthralgia. Patients with CF very often present arthralgia and impairment of the neuromuscular function, causing a debilitating condition which contributes to the burden of disease (28). Consistently, using survivor animals, we observed that sofosbuvir protected CHIKV-infected mice form neuromotor sequalae when compared to untreated animals. Under this behaviour test, it is likely that both direct neuromotor sequelae and/or problems on mice articulations may contributed to the high time required for CHIKV-infected animals to turn from back to upright position.

Altogether, our data reveals that CHIKV is susceptible to sofosbuvir, highlighting that other genetically distinct and clinically important viruses phylogenetically distributed among members of the Togaviridae and Flaviviridae families could also be susceptible to this drug. Wider use of sofosbuvir, beyond HCV, may represent a safer antiviral option than ribavirin. Finally, in the context of this study, our findings motivate phase II clinical investigations on the new use of sofosbuvir as treatment against CHIKV.

bioRxiv preprint doi: https://doi.org/10.1101/360305; this version posted July 2, 2018. The copyright holder for this preprint (which was not certified by peer review) is the author/funder, who has granted bioRxiv a license to display the preprint in perpetuity. It is made available under aCC-BY-NC-ND 4.0 International license.

4. Material and Methods

Reagents. The antiviral sofosbuvir (β-d-2'-deoxy-2'-α-fluoro-2'-β-C-methyluridine) was donated by the BMK Consortium: Blanver Farmoquímica Ltda; Microbiológica Química e Farmacêutica Ltda; Karin Bruning & Cia. Ltda, (Taboão da Serra, São Paulo, Brazil). Ribavirin was received as a donation from the Instituto de Tecnologia de Farmacos (Farmanguinhos, Fiocruz). All small molecule inhibitors were dissolved in 100 % dimethylsulfoxide (DMSO) and subsequently diluted at least 10^4-fold in culture or reaction medium before each assay. The final DMSO concentrations showed no cytotoxicity. The materials for cell culture were purchased from Thermo Scientific Life Sciences (Grand Island, NY), unless otherwise mentioned.

Cells. African green monkey kidney (Vero) and human hepatoma (Huh-7) cells were cultured in DMEM. The culture medium of each cell type was supplemented with 10 % fetal bovine serum (FBS; HyClone, Logan, Utah), 100 U/mL penicillin, and 100 µg/mL streptomycin(38, 39) at 37 °C in 5 % CO_2.

Virus. CHIKV (Asian strain) was donated by Dr. Amilcar Tanuri. CHIKV was propagated in Vero cells at a multiplicity of infection (MOI) of 0.1. Infection was carried out for 1 h at 37 °C. Next, the residual virus particles were removed by washing with phosphate-buffered saline (PBS), and the cells were cultured for an additional 2 to 5 days. After each period, the cells were lysed by freezing and thawing and centrifuged at 1,500 x *g* at 4 °C for 20 min to remove cellular debris. Virus titters were determined by classical 10-fold dilution and tissue cytopathic infectious dose 50 ($TCID_{50}$)/mL calculation.

Cytotoxicity assay. Monolayers of cells 2 to 5 x 10^4 cells/well in 96-well plates were treated for 5 days with various concentrations of sofosbuvir or ribavirin as a control. Then, 5 mg/ml 2,3-bis-(2-methoxy-4-nitro-5-sulfophenyl)-2*H*-tetrazolium-5-carboxanilide (XTT) in DMEM was added to the cells in the presence of 0.01 % of N-methyl dibenzopyrazine methyl sulfate (PMS). After incubating for 4 h at 37 °C, the plates

bioRxiv preprint doi: https://doi.org/10.1101/360305; this version posted July 2, 2018. The copyright holder for this preprint (which was not certified by peer review) is the author/funder, who has granted bioRxiv a license to display the preprint in perpetuity. It is made available under aCC-BY-NC-ND 4.0 International license.

were read in a spectrophotometer at 492 nm and 620 nm (40). The 50 % cytotoxic concentration (CC_{50}) was calculated by a non-linear regression analysis of the dose–response curves.

Yield-reduction assay. Monolayers of 5 x 10^4 Huh-7 cells/well in 96-well plates were infected with CHIKV at the MOI of 0.1 for 1 h at 37 °C. The cells were washed with PBS to remove residual viruses, and various concentrations of sofosbuvir, or ribavirin as a positive control, in DMEM with 1 % FBS were added. After 24 h, the cells were lysed, the cellular debris was cleared by centrifugation, and the virus titers in the supernatant were determined in Vero cells as $TCID_{50}$/mL. A non-linear regression analysis of the dose-response curves was performed to calculate the concentration at which each drug inhibited the plaque-forming activity of CHIKV by 50 % (EC_{50}).

Generation of human iPSC-derived astrocytes lines. Astrocytes were differentiated from neural stem cells (NSC), 20 x 10^3 cells/well in a 96-well plate, obtained from human iPSC of three control cell lines from healthy subjects (41). These cell lines were previously used in other studies from our research group (16). Three cell lines from healthy subjects were obtained from a female subject (GM23279A, available at Coriell Institute - coriell.org) and the other two from male subjects from cells reprogrammed at the D'Or Institute for Research and Education (CF1 & CF2). NSCs were differentiated into astrocytes as described in Yan, 2013 (42). Briefly, NSCs were cultured in differentiation media (1% N2 supplement and 1% FBS in DMEM/F12) for 21 days with media changes every other day and passages every week. After this period, glial cells were grown for 5 weeks in 10% FBS in DMEM/F12 with media changes twice a week prior to use. Cells were infected at MOIs of either 1.0 or 10 for 2 h at 37 °C. Next, the cells were washed, and fresh medium containing sofosbuvir was added. The cells were treated daily with sofosbuvir at the indicated concentrations. Virus titers were determined from the culture supernatant. Cell death was measured by adding 2 µM CellEvent caspase-3/7 reagent and the fluorescent dye ethidium homodimer (43), when the culture supernatants were collected, on the 5th day after infection. Images were acquired with an Operetta high-content imaging system with a 20x objective and high numerical apertures (NA) (PerkinElmer, USA). The data were analyzed using the high-content image analysis software Harmony 5.1 (PerkinElmer, USA). Seven independent fields were evaluated from triplicate wells per experimental condition.

bioRxiv preprint doi: https://doi.org/10.1101/360305; this version posted July 2, 2018. The copyright holder for this preprint (which was not certified by peer review) is the author/funder, who has granted bioRxiv a license to display the preprint in perpetuity. It is made available under aCC-BY-NC-ND 4.0 International license.

3D Modeling of the Chikungunya Virus Nonstructural Protein 4. The amino acid sequence of the nonstructural protein 4 (NSP4) of chikungunya virus (CHIKV, UniProtKB ID: F2YI10) was obtained from ExPASy server (44). The region between Met1-Lys516, part of the nsP4 sequence that includes the whole catalytic core was considered to construct the model using I-TASSER server (45). The I-TASSER methodology is very accurate for the construction of protein models when the sequence identity between the target sequence and the template protein drops below 30 %, where lack of a high-quality structure match may provide substantial alignment errors and, consequently, poor quality models (45, 46). Thus, the final model was validated using two programs: PROCHECK (47) and VERIFY3D (48). PROCHECK analyzes the stereochemical quality and VERIFY3D compatibility analysis between the 3D model and its own amino acid sequence, by assigning a structural class based on its location and environment, and by comparing the results with those of crystal structures with good resolutions (47, 48).

Molecular Docking. The structures of SFV and UTP were built in the Spartan'14 software (Wavefunction, Inc., Irvine, CA). The docking of the two ligands to the nsP4 model was performed using Molegro Virtual Docker 6.0 (MVD) program (CLC bio, Aarhus, Denmark) (21), which uses a heuristic search algorithm that combines differential evolution with a cavity prediction algorithm (21). The MolDock scoring function used is based on a modified piecewise linear potential (PLP) with new hydrogen bonding and electrostatic terms included. The full description of the algorithm and its reliability compared to other common docking algorithm have been described (21). The two Mg^{2+} ions were set as the center of searching space with a radius value of 10 Å. In addition, the search algorithm MolDock optimizer was used with a minimum of 100 runs and the parameter settings were population size = 500; maximum iteration = 2000; scaling factor = 0.50; offspring scheme = scheme 1; termination scheme = variance-based; crossover rate = 0.90. Due to the stochastic nature of algorithm search, three independent simulations per ligand were performed to predict the binding mode. Consequently, the complexes with the lowest interaction energy were evaluated. The interactions between nsP4 model and each ligand were analyzed using the ligand map algorithm, a standard

bioRxiv preprint doi: https://doi.org/10.1101/360305; this version posted July 2, 2018. The copyright holder for this preprint (which was not certified by peer review) is the author/funder, who has granted bioRxiv a license to display the preprint in perpetuity. It is made available under aCC-BY-NC-ND 4.0 International license.

algorithm in MVD program (21). The usual threshold values for hydrogen bonds and steric interactions were used.

All figures of nsP4 modeling and molecular docking results were edited using Visual Molecular Dynamics 1.9.3 (VMD) program (available for download at http://www.ks.uiuc.edu/Research/vmd/vmd-1.9.3/) (49).

Animals. Swiss albino mice (*Mus musculus*) (pathogen-free) from the Oswaldo Cruz Foundation breeding unit (Instituto de Ciência e Tecnologia em Biomodelos (ICTB)/Fiocruz) were used for these studies. The animals were kept at a constant temperature (25°C) with free access to chow and water in a 12-h light/dark cycle. The experimental laboratory received pregnant mice (at approximately the 14th gestational day) from the breeding unit. Pregnant mice were observed daily until delivery to accurately determine the postnatal day. We established a litter size of 10 animals for all experimental replicates.

The Animal Welfare Committee of the Oswaldo Cruz Foundation (CEUA/FIOCRUZ) approved and covered (license numbers L-016/2016 and CEUA L-002/2018) the experiments in this study. The procedures described in this study were in accordance with the local guidelines and guidelines published in the National Institutes of Health Guide for the Care and Use of Laboratory Animals. The study is reported in accordance with the ARRIVE guidelines for reporting experiments involving animals(50). If necessary to alleviate animal suffering, euthanasia was performed. The criteria were the following: i) differences in weight gain between infected and control groups >50%, ii) ataxia, iii) loss of gait reflex, iv) absence of righting reflex within 60 seconds, and v) separation, with no feeding, of moribund offspring by the female adult mouse.

Experimental infection and treatment.

Neonate model. Three-day-old Swiss mice were infected intraperitoneally with 2 x 10^2 $TCID_{50}$ of virus(51, 52), unless otherwise mentioned. Treatments with sofosbuvir were carried out with sofosbuvir at 20 mg/kg/day intraperitoneally. Treatment started one day prior to infection (pretreatment) or two days after infection (late treatment). In both cases, treatment was conducted for 6 days. For comparisons, mock-

bioRxiv preprint doi: https://doi.org/10.1101/360305; this version posted July 2, 2018. The copyright holder for this preprint (which was not certified by peer review) is the author/funder, who has granted bioRxiv a license to display the preprint in perpetuity. It is made available under aCC-BY-NC-ND 4.0 International license.

infected and mock-treated groups of animals were used as controls. Animals were monitored daily for survival, weight gain, and virus-induced short-term sequelae (righting in up to 60 seconds).

Arthralgia model. Arthralgia model was adapted from previous publications (53, 54). Male Swiss Webster mice (8 weeks-old; 20-25 g) were infected with 10^4 $TCID_{50}$ in right hind paw towards the ankle. Sofosbuvir was given orally (20 mg/kg), beginning one-hour before the first virus injection. Treatment was conducted for 6 days. Control group was injected with 50 µL of RPMI. Paw oedema was evaluated from the first to the sixth day after infection by hydropletismometer for small volumes (Ugo Basile, Milan, Italy) and data was presented as paw volume (mL).

Behavioural tests. To test the righting reflex, animals were tested daily during the course of acute infection. Animals were held in a supine position with all four paws facing up in the air for 5 seconds. Then, animals were released, and the time the animal took to flip over onto its stomach with all four paws touching the surface was measured. A maximum of 60 seconds was given for each trial, and animals were tested twice a day with a 5-minute minimum interval between trials. For each animal, the lowest time was plotted in the graph. Animals that failed the test were included in the graph with a time of 60 seconds.

Statistical analysis. All assays were performed and codified by one professional. Subsequently, a different professional analyzed the results before the identification of the experimental groups. This approach was used to keep the pharmacological assays blind. All experiments were carried out at least three independent times, including technical replicates in each assay. The dose-response curves used to calculate the EC_{50} and CC_{50} values were generated by Excel for Windows. The dose-response curves used to calculate the IC_{50} values were produced by Prism GraphPad software 5.0. Significance of survival curves was evaluated using the Log-rank (Mantel-Cox) test. The equations to fit the best curve were generated based on R^2 values ≥ 0.9. ANOVA, followed by Tukey's post hoc test, tests were also used, with P values <0.05 considered statistically significant. The statistical analyses specific to each software program used in the bioinformatics analysis are described above.

bioRxiv preprint doi: https://doi.org/10.1101/360305; this version posted July 2, 2018. The copyright holder for this preprint (which was not certified by peer review) is the author/funder, who has granted bioRxiv a license to display the preprint in perpetuity. It is made available under aCC-BY-NC-ND 4.0 International license.

References

1. Pialoux G, gilles.pialoux@tnn.aphp.fr, Hôpital Tenon SdMIeT, Paris, France, Gaüzère B-A, CHD de Saint-Denis LR, France, Jauréguiberry S, et al. Chikungunya, an epidemic arbovirosis. The Lancet Infectious Diseases. 2007;7(5):319-27.
2. Pinheiro TJ, Hospital dos Servidores do Estado RdJ, Brasil, Hospital dos Servidores do Estado RdJ, Brasil, Guimarães LF, Hospital dos Servidores do Estado RdJ, Brasil, Hospital dos Servidores do Estado RdJ, Brasil, et al. Neurological manifestations of Chikungunya and Zika infections. Arq Neuro-Psiquiatr. 2016;74(11):937-43.
3. Parra B, Lizarazo J, Jiménez-Arango JA, Zea-Vera AF, González-Manrique G, Vargas J, et al. Guillain–Barré Syndrome Associated with Zika Virus Infection in Colombia. https://doiorg/101056/NEJMoa1605564. 2016.
4. Prevention C-CfDCa. Geographic Distribution | Chikungunya virus | CDC. 2018.
5. Souza TMA, Viral Immunology Laboratory OCI, Rio de Janeiro, Brazil, Azeredo EL, Viral Immunology Laboratory OCI, Rio de Janeiro, Brazil, Badolato-Corrêa J, Viral Immunology Laboratory OCI, Rio de Janeiro, Brazil, et al. First Report of the East-Central South African Genotype of Chikungunya Virus in Rio de Janeiro, Brazil. PLOS Currents Outbreaks. 2018.
6. Charlys da Costa A, Thézé J, Komninakis SCV, Sanz-Duro RL, Felinto MRL, Moura LCC, et al. Spread of Chikungunya Virus East/Central/South African Genotype in Northeast Brazil. Emerg Infect Dis. 232017. p. 1742-4.
7. Nunes MRT, Faria NR, Vasconcelos JMd, Golding N, Kraemer MU, Oliveira LFd, et al. Emergence and potential for spread of Chikungunya virus in Brazil. BMC Medicine. 2015;13(1):102.
8. Strauss JH, Strauss EG. The alphaviruses: gene expression, replication, and evolution. Microbiol Rev. 1994;58(3):491-562.
9. Chen MW, Tan YB, Zheng J, Zhao Y, Lim BT, Cornvik T, et al. Chikungunya virus nsP4 RNA-dependent RNA polymerase core domain displays detergent-sensitive primer extension and terminal adenylyltransferase activities. Antiviral Res. 2017;143:38-47.
10. Gohara DW, Crotty S, Arnold JJ, Yoder JD, Andino R, Cameron CE. Poliovirus RNA-dependent RNA polymerase (3Dpol): structural, biochemical, and biological analysis of conserved structural motifs A and B. J Biol Chem. 2000;275(33):25523-32.
11. Bhatia HK, Singh H, Grewal N, Natt NK. Sofosbuvir: A novel treatment option for chronic hepatitis C infection. J Pharmacol Pharmacother. 2014;5(4):278-84.
12. Gilead. Product Monograph Pr SOVALDI® (sofosbuvir) Tablets 400 mg sofosbuvir Antiviral Agent 2015 [Available from: http://www.gilead.com/-/media/8c41933bdd5d4e4691af495f40aa6016.ashx.
13. European Medicines Agency, EMA. Sovaldi 2013 [Available from: http://www.ema.europa.eu/docs/en_GB/document_library/EPAR__Public_assessment_report/human/002798/WC500160600.pdf.
14. Ferreira AC, Zaverucha-do-Valle C, Reis PA, Barbosa-Lima G, Vieira YR, Mattos M, et al. Sofosbuvir protects Zika virus-infected mice from mortality, preventing short- and long-term sequelae. Scientific Reports. 2017;7(1):9409.
15. Bullard-Feibelman KM, Govero J, Zhu Z, Salazar V, Veselinovic M, Diamond MS, et al. The FDA-approved drug sofosbuvir inhibits Zika virus infection. Antiviral Res. 2017;137:134-40.
16. Sacramento CQ, de Melo GR, de Freitas CS, Rocha N, Hoelz LV, Miranda M, et al. The clinically approved antiviral drug sofosbuvir inhibits Zika virus replication. Sci Rep. 2017;7:40920.
17. Onorati M, Li Z, Liu F, Sousa AM, Nakagawa N, Li M, et al. Zika virus disrupts phospho-TBK1 localization and mitosis in human neuroepithelial stem cells and radial glia. Cell Rep. 2016;16(10):2576-92.
18. Freitas Cd, Higa L, Sacramento C, Ferreira A, Reis P, Delvecchio R, et al. Yellow fever virus is susceptible to sofosbuvir both in vitro and in vivo. 2018.
19. Xu H-T, Colby-Germinario SP, Hassounah SA, Fogarty C, Osman N, Palanisamy N, et al. Evaluation of Sofosbuvir (β-D-2′-deoxy-2′-α-fluoro-2′-β-C-methyluridine) as an inhibitor of Dengue virus replication #. Scientific Reports. 2017;7(1):6345.
20. Vicenti I, Boccuto A, Giannini A, Dragoni F, Saladini F, Zazzi M. Comparative analysis of different cell systems for Zika virus (ZIKV) propagation and evaluation of anti-ZIKV compounds in vitro. Virus Res. 2018;244:64-70.
21. Thomsen R, Christensen MH. MolDock: a new technique for high-accuracy molecular docking. J Med Chem. 2006;49(11):3315-21.
22. Ganesan VK, Duan B, Reid SP. Chikungunya Virus: Pathophysiology, Mechanism, and Modeling. Viruses. 2017;9(12).

bioRxiv preprint doi: https://doi.org/10.1101/360305; this version posted July 2, 2018. The copyright holder for this preprint (which was not certified by peer review) is the author/funder, who has granted bioRxiv a license to display the preprint in perpetuity. It is made available under aCC-BY-NC-ND 4.0 International license.

603 23. MASON PJ, HADDOW AJ. An epidemic of virus disease in Southern Province, Tanganyika Territory, in 1952-
604 53; an additional note on Chikungunya virus isolations and serum antibodies. Trans R Soc Trop Med Hyg.
605 1957;51(3):238-40.
606 24. Weaver SC. Arrival of Chikungunya Virus in the New World: Prospects for Spread and Impact on Public
607 Health. PLoS Negl Trop Dis. 2014;8(6).
608 25. Krishnamoorthy K, Harichandrakumar KT, Krishna Kumari A, Das LK. Burden of chikungunya in India:
609 estimates of disability adjusted life years (DALY) lost in 2006 epidemic. J Vector Borne Dis. 2009;46(1):26-35.
610 26. Saúde SdVe, Saúde Md. Monitoramento dos casos de dengue, febre de chikungunya e febre pelo vírus Zika
611 até a Semana Epidemiológica 8 de 2018: Ministerio da Saude; 2018 [Available from:
612 http://portalarquivos2.saude.gov.br/images/pdf/2018/marco/29/2018-010.pdf.

613 27. World Health Organization ROfS-EA. Guidelines on clinical management of chikungunya fever [Publications].
614 WHO Regional Office for South-East Asia; 2008 [updated 2008. Available from:
615 http://apps.who.int/iris/handle/10665/205178.
616 28. Gasque P, UMR PIMIT PIeMITUdLR, INSERM U1187, CNRS 9192, IRD 249, St. Denis, France, Bandjee MCJ,
617 UMR PIMIT PIeMITUdLR, INSERM U1187, CNRS 9192, IRD 249, St. Denis, France, Reyes MM, National Health Institute
618 PHRD, Bogotá, et al. Chikungunya Pathogenesis: From the Clinics to the Bench. The Journal of Infectious Diseases.
619 2018;214(suppl_5).
620 29. Abdelnabi R, Neyts J, Delang L. Towards antivirals against chikungunya virus. Antiviral Res. 2015;121:59-68.
621 30. Varghese FS, Kaukinen P, Gläsker S, Bespalov M, Hanski L, Wennerberg K, et al. Discovery of berberine,
622 abamectin and ivermectin as antivirals against chikungunya and other alphaviruses. Antiviral Res. 2016;126:117-24.
623 31. Mastrangelo E, Pezzullo M, De Burghgraeve T, Kaptein S, Pastorino B, Dallmeier K, et al. Ivermectin is a
624 potent inhibitor of flavivirus replication specifically targeting NS3 helicase activity: new prospects for an old drug. J
625 Antimicrob Chemother. 2012;67(8):1884-94.
626 32. Das PK, Merits A, Lulla A. Functional cross-talk between distant domains of chikungunya virus non-structural
627 protein 2 is decisive for its RNA-modulating activity. J Biol Chem. 2014;289(9):5635-53.
628 33. Varghese FS, Thaa B, Amrun SN, Simarmata D, Rausalu K, Nyman TA, et al. The Antiviral Alkaloid Berberine
629 Reduces Chikungunya Virus-Induced Mitogen-Activated Protein Kinase Signaling. J Virol. 2016;90(21):9743-57.
630 34. Inglis FM, Lee KM, Chiu KB, Purcell OM, Didier PJ, Russell-Lodrigues K, et al. Neuropathogenesis of
631 Chikungunya Infection: Astrogliosis and Innate Immune Activation. J Neurovirol. 2016;22(2):140-8.
632 35. Brizzi K. Neurologic Manifestation of Chikungunya Virus | SpringerLink. 2018.
633 36. Ferreira A, Valle C, Reis P, Barbosa-Lima G, Vieira Y, Mattos M, et al. Sofosbuvir protects Zika virus-
634 infected mice from mortality, preventing short- and long-term sequela. bioRxiv 2017.
635 37. Muthuri SG, Venkatesan S, Myles PR, Leonardi-Bee J, Al Khuwaitir TS, Al Mamun A, et al. Effectiveness of
636 neuraminidase inhibitors in reducing mortality in patients admitted to hospital with influenza A H1N1pdm09 virus
637 infection: a meta-analysis of individual participant data. Lancet Respir Med. 2014;2(5):395-404.
638 38. Li GY, Li BG, Yang T, Liu GY, Zhang GL. Chaetoindicins A-C, three isoquinoline alkaloids from the fungus
639 Chaetomium indicum. Org Lett. 2006;8(16):3613-5.
640 39. Zhang H, Wang YF, Shen CH, Agniswamy J, Rao KV, Xu CX, et al. Novel P2 tris-tetrahydrofuran group in
641 antiviral compound 1 (GRL-0519) fills the S2 binding pocket of selected mutants of HIV-1 protease. J Med Chem.
642 2013;56(3):1074-83.
643 40. Scudiero DA, Shoemaker RH, Paull KD, Monks A, Tierney S, Nofziger TH, et al. Evaluation of a soluble
644 tetrazolium/formazan assay for cell growth and drug sensitivity in culture using human and other tumor cell lines.
645 Cancer Res. 1988;48(17):4827-33.
646 41. Garcez PP, Loiola EC, Madeiro da Costa R, Higa LM, Trindade P, Delvecchio R, et al. Zika virus impairs growth
647 in human neurospheres and brain organoids. Science. 2016.
648 42. Yan Y, Shin S, Jha BS, Liu Q, Sheng J, Li F, et al. Efficient and rapid derivation of primitive neural stem cells and
649 generation of brain subtype neurons from human pluripotent stem cells. Stem Cells Transl Med. 2013;2(11):862-70.
650 43. Sauter NK, Hanson JE, Glick GD, Brown JH, Crowther RL, Park SJ, et al. Binding of influenza virus
651 hemagglutinin to analogs of its cell-surface receptor, sialic acid: analysis by proton nuclear magnetic resonance
652 spectroscopy and X-ray crystallography. Biochemistry. 1992;31(40):9609-21.
653 44. Gasteiger E, Gattiker A, Hoogland C, Ivanyi I, Appel RD, Bairoch A. ExPASy: The proteomics server for in-depth
654 protein knowledge and analysis. Nucleic Acids Res. 2003;31(13):3784-8.
655 45. Yang J, Yan R, Roy A, Xu D, Poisson J, Zhang Y. The I-TASSER Suite: protein structure and function prediction.
656 Nat Methods. 2015;12(1):7-8.

bioRxiv preprint doi: https://doi.org/10.1101/360305; this version posted July 2, 2018. The copyright holder for this preprint (which was not certified by peer review) is the author/funder, who has granted bioRxiv a license to display the preprint in perpetuity. It is made available under aCC-BY-NC-ND 4.0 International license.

46. Gazos-Lopes F, Oliveira MM, Hoelz LV, Vieira DP, Marques AF, Nakayasu ES, et al. Structural and functional analysis of a platelet-activating lysophosphatidylcholine of Trypanosoma cruzi. PLoS Negl Trop Dis. 2014;8(8):e3077.
47. R. A. Laskowski MWM, D. S. Moss and J. M. Thornton, TI. PROCHECK: a program to check the stereochemical quality of protein structures. Journal of Applied Crystallography. 1993;26(2):283-91.
48. Eisenberg D, Lüthy R, Bowie JU. VERIFY3D: assessment of protein models with three-dimensional profiles. Methods Enzymol. 1997;277:396-404.
49. Humphrey W, Dalke A, Schulten K. VMD: visual molecular dynamics. J Mol Graph. 1996;14(1):33-8, 27-8.
50. Kilkenny C, Browne WJ, Cuthill IC, Emerson M, Altman DG. Improving bioscience research reporting: the ARRIVE guidelines for reporting animal research. Osteoarth Cartil. 2012;20(4):256-60.
51. van den Pol AN, Mao G, Yang Y, Ornaghi S, Davis JN. Zika virus targeting in the developing brain. J Neurosci. 2017;37(8):2161-75.
52. Huang WC, Abraham R, Shim BS, Choe H, Page DT. Zika virus infection during the period of maximal brain growth causes microcephaly and corticospinal neuron apoptosis in wild type mice. Sci Rep. 2016;6:34793.
53. Hawman DW, Stoermer KA, Montgomery SA, Pal P, Oko L, Diamond MS, et al. Chronic joint disease caused by persistent Chikungunya virus infection is controlled by the adaptive immune response. J Virol. 2013;87(24):13878-88.
54. Gardner J, Anraku I, Le TT, Larcher T, Major L, Roques P, et al. Chikungunya virus arthritis in adult wild-type mice. J Virol. 2010;84(16):8021-32.

AUTHOR CONTRIBUTIONS

Performed the experiments – ACF, PAR, CSdeF, CQS, LVBH, MMB, MM, ECL, PT, YRV, GB-L

Conceptualized the experiments and fund raising – HCCFN, NB, SKR, KB, FAB, PTB, TMLS

Provided critical material – KB

Study organization - TMLS

All authors revised and approved the manuscript.

Financial Support

Funders had no role in the experiment design or interpretation

Acknowledgements

Funding was provided by National Council for Scientific and Technological Development (CNPq), Ministry of Science, Technology, Information and Communications (grants including, but not limited to, # 465313/2014-0; Ministry of Education/CAPES (# 465313/2014-0); Research Foundation of the State of Rio de Janeiro (FAPERJ) (grants including, but not limited to, # 465313/2014-0 and Oswaldo Cruz Foundation (Fiocruz).

Conflict of Interest

bioRxiv preprint doi: https://doi.org/10.1101/360305; this version posted July 2, 2018. The copyright holder for this preprint (which was not certified by peer review) is the author/funder, who has granted bioRxiv a license to display the preprint in perpetuity. It is made available under aCC-BY-NC-ND 4.0 International license.

693 A competing financial interest exists for KB, who is partner in a consortium able to produce generic
694 sofosbuvir. The consortium and her participation was limited to provide the sofosbuvir for this study.

695

696

697

698

699

700

701

702

703

704

705

706

707

708

709

710

711

712